photonics

Article

Four-Wave Optical Parametric Amplification in a Raman-Active Gas

Yuichiro Kida [1,*] and Totaro Imasaka [1,2]

[1] Department of Applied Chemistry, Graduate School of Engineering, Kyushu University, 744 Motooka, Nishi-ku, Fukuoka 819-0395, Japan; E-Mail: imasaka@cstf.kyushu-u.ac.jp

[2] Division of Optoelectronics and Photonics, Center for Future Chemistry, Kyushu University, 744 Motooka, Nishi-ku, Fukuoka 819-0395, Japan

* Author to whom correspondence should be addressed; E-Mail: y-kida@cstf.kyushu-u.ac.jp; Tel.: +81-92-802-2886; Fax: +81-92-802-2888.

Abstract: Four-wave optical parametric amplification (FWOPA) in a Raman-active medium is experimentally investigated by use of an air-filled hollow fiber. A femtosecond pump pulse shorter than the period of molecular motion excites the coherent molecular motion of the Raman-active molecules during the parametric amplification of a signal pulse. The excited coherent motion modulates the frequency of the signal pulse during the parametric amplification, and shifts it to lower frequencies. The magnitude of the frequency redshift depends on the pump intensity, resulting in intensity-dependent spectral characteristics that are different from those in the FWOPA induced in a noble-gas-filled hollow fiber.

Keywords: four-wave mixing; optical parametric amplification

1. Introduction

Nonlinear optical effects have been investigated in various media for broadband light amplification. In particular, the optical parametric amplification via the second-order nonlinearity of a birefringent crystal has allowed broadband light amplification supporting sub-10-fs pulses in the visible and infrared wavelength regions [1,2]. The amplification bandwidth is further extended by the multi-wavelength pumping scheme [3,4]. The high amplification gain reached by the parametric amplification has led to the generation of sub-10-fs optical pulses with terawatt peak powers [5,6]. Such a highly intense pulse has been applied to initiate the relativistic light-matter interaction generating monoenergetic electrons [7].

The parametric amplification based on third-order nonlinearity, nonresonant four-wave optical parametric amplification (FWOPA), also amplifies light in a broad spectral range [8–11]. An amplification gain as high as 100 has been reached in bulk media such as water and glasses [8,9]. By the use of a picosecond pump pulse, amplification up to a submillijoule pulse energy has been demonstrated [8,9]. The use of a gaseous medium has also led to an amplification gain that is similar to those in bulk media as well as a broad amplification bandwidth supporting a sub-10-fs pulse duration [11]. In the scheme of the FWOPA, self-phase modulation (SPM) and cross-phase modulation (XPM) simultaneously induced by an intense pump pulse significantly alter the phase matching condition by the induction of the nonlinear phase mismatch. It modifies the wavelength dependence of the amplification gain to what is not predicted by the linear phase mismatch.

When a Raman-active gas medium and a pump pulse that is shorter than the period of molecular motion (vibration or rotation) are utilized in the FWOPA, it is expected that the coherent molecular motion is impulsively excited by the pump pulse via impulsive stimulated Raman scattering [12]. Such coherent motion induces the ultrafast variation of the refractive index of the medium, modulating the frequency of a laser pulse with an arbitrary wavelength copropagating with the pump pulse [13] as well as that of the pump pulse [13–16]. The coherent molecular motion is also expected to have effects on the amplification characteristics of the FWOPA. It has, to our knowledge, not been experimentally investigated how the coherent motion alters the amplification characteristics of the signal pulse being amplified via the FWOPA induced in a Raman-active gas.

In this research, the effect of coherent molecular motion on the signal amplification via the FWOPA is investigated by use of an air-filled hollow fiber. A femtosecond pump pulse impulsively excites coherent molecular rotations or coherent rotational wavepackets [15,16] during the FWOPA. The wavepackets modulate the frequency of the signal pulse being amplified, leading to a continuously redshifted spectrum of the amplified signal pulse. The amplification characteristics in the Raman-active medium are different from those of the FWOPA induced in a noble-gas filled hollow fiber.

2. Theoretical Background

In the degenerate FWOPA, two input pulses, a pump pulse (p) and a signal pulse (s), generate an idler pulse (i) via the degenerate four-wave mixing (FWM) for which the energy conservation law of $\omega_i = 2\omega_p - \omega_s$ is satisfied, where ω_l is the angular frequency of each pulse. During the interaction of the FWM, the signal pulse is parametrically amplified by the energy transfer from the pump pulse to the signal pulse [8–11]. In addition, the pump pulse induces nonlinear refractive index in the medium, which in the case of a Raman-inactive medium like a noble gas, originates from the instantaneous response of the bound electrons. The induced nonlinear refractive index is proportional to the intensity of the pump laser pulse, I_p, as: $\Delta n_{\mathrm{ele}}(t) = n_{2,\mathrm{ele}} I_p(t) = (3\chi_{\mathrm{ele}}^{(3)}/8n)|A_p(t)|^2$, where the electric field of a laser pulse is assumed to be expressed as $E_l(z,t) = (1/2)A_l \exp[i(\beta_l z - \omega_l t)] + c.c.$, with the slowly-varying amplitude, $A_l(t)$, propagation constant, β_l, and angular frequency, ω_l, respectively. n, $n_{2,\mathrm{elec}}$, and $\chi_{\mathrm{ele}}^{(3)}$ stand for the linear refractive index, nonlinear refractive index coefficient, and the corresponding third-order susceptibility, respectively. The phase modulation arising from the induced nonlinear refractive index alternates the amplification behavior of the signal pulse in the FWOPA [11,17].

In case of the FWOPA in a Raman-active medium, nonlinear response originating from coherent molecular vibration and rotation needs to be taken into account. A pump pulse propagating through a Raman-active medium impulsively excites coherent molecular motion when the duration of the pump pulse is shorter than the period of the motion [12,13]. The excited molecular coherence leads to the nonlinear change in the refractive index, $\Delta n_{2,\text{nuc}}(t)$, whose response is not instantaneous. In case of molecular vibration, the magnitude of the noninstantaneous nonlinear response depends on the vibrational coordinate Q which grows within the pump pulse as [13]: $Q \approx \frac{\varepsilon_0}{4M}\left(\frac{\partial \alpha}{\partial Q}\right)\int_0^t dt'\int_0^t dt'' \mid A_p(t'')\mid^2$, where ε_0, M, $\left(\frac{\partial \alpha}{\partial Q}\right)$, and $A_p(t)$ are the permittivity of free space, the effective mass, the differential polarizability, and the slowly varying envelope of the pump pulse, respectively. The induced nonlinear refractive index, $\Delta n_{2,\text{nuc}}$, is expressed by $\frac{N}{2n}\left(\frac{\partial \alpha}{\partial Q}\right)Q$, where N is the density of the medium. For molecular rotation, on the other hand, the induced nonlinear refractive index is expressed by $\Delta n_{nuc}(t) = \int_0^\infty R(t')I_p(t-t')dt'$ [18,19], with the following response function $R(t)$ [18,19]: $R(t) = \frac{32\pi^2 N}{hcn}[\alpha_\parallel(\omega) - \alpha_\perp(\omega)]^2 \sum_{J=0}^\infty [\rho_{J+2} - \rho_J]Z_J \frac{(J+2)(J+1)}{2J+3}\sin(-\omega_J t)$. $\alpha_\parallel(\omega)$ and $\alpha_\perp(\omega)$, respectively, are the polarizability along the symmetry axis of the molecules and that along the axis perpendicular to the symmetry axis. ρ_J is the population of the rotational level J, and Z_J is the constant that takes into account the quantum effects of nuclear statistics. The response function contains the angular frequency difference between the coupled rotational levels, $\omega_J = 4\pi Bc(2J+3)$ [19].

In both cases of molecular vibration and rotation, the frequency of the pump pulse redshifts during the excitation of coherent molecular vibration [13,14] or rotation [19]. This arises from the delayed nuclear response $\Delta n_{2,\text{nuc}}(t)$ originating from the coherent molecular vibration or rotation induced by the pump pulse. When another laser pulse copropagates with the pump pulse, the frequency of the laser pulse is also modulated by the similar manner as the pump pulse. Under the presence of such nuclear response, the coupled equations for the propagation of the pump, signal, and idler pulses for the degenerate, nonresonant FWOPA [11] may be written as:

$$\frac{\partial A_p}{\partial z} = i\frac{\omega_p}{c}\left[\left\{\Delta n_{2,ele} + \Delta n_{2,\text{nuc}}\right\}A_p + \frac{3\chi_{\text{ele}}^{(3)}}{4n_p}A_p^* A_i A_s \exp(i\Delta\beta z)\right] \tag{1}$$

$$\frac{\partial A_{s,i}}{\partial z} = i\frac{\omega_{s,i}}{c}\left[\left\{2\Delta n_{2,ele} + \Delta n_{2,\text{nuc}}\right\}A_{s,i} + \frac{3\chi_{\text{ele}}^{(3)}}{8n_{s,i}}A_p^2 A_{i,s}^* \exp(-i\Delta\beta z)\right] \tag{2}$$

under the slowly varying envelop approximation [20]. $\Delta\beta$ is the linear phase mismatch ($\Delta\beta = \beta_s + \beta_i - 2\beta_p$) which dominates the efficiency of the parametric amplification. The intensities of the signal and idler pulses are assumed to be too low to induce the electronic Kerr effect, as is the case in the experiments described below. The first terms on the right sides of Equations (1) and (2) relate to SPM and XPM resulting from the response of the bound electrons, and the third terms account for the degenerate FWM. The second terms on the right sides of the equations are related to the delayed nuclear response to the fields, originating from the coherent vibration or rotation. In the case of the FWOPA in a Raman-active medium, the nonlinear refractive index originating from the delayed nuclear response is expected to

result in a continuous spectral redshift of the pump pulse, which is related to the second term in Equation (1). When the signal and idler pulses copropagate with the pump pulse, these laser pulses should experience the similar spectral redshift. The simultaneous phase modulation by the coherent motion (the second term) and the parametric amplification (the third term in Equation (2)), therefore, result in a spectral redshift of the signal spectrum during the parametric amplification. This is schematically explained in Figure 1b. The magnitude of the redshift depends on the induced nonlinear refractive index, and hence, a medium with a large Raman gain coefficient leads to a large spectral redshift. In case of a Raman-inactive medium, on the other hand, the second terms on the right sides of the coupled equations are missing and the signal pulse is solely phase modulated by the SPM and XPM induced by the instantaneous response of the bound electrons. The frequency of the signal pulse is modulated to both higher and lower frequencies, and the center of gravity of the spectrum remains unchanged as is schematically drawn in Figure 1a. The spectral red-shift is hence expected to be observed only in a Raman-active medium.
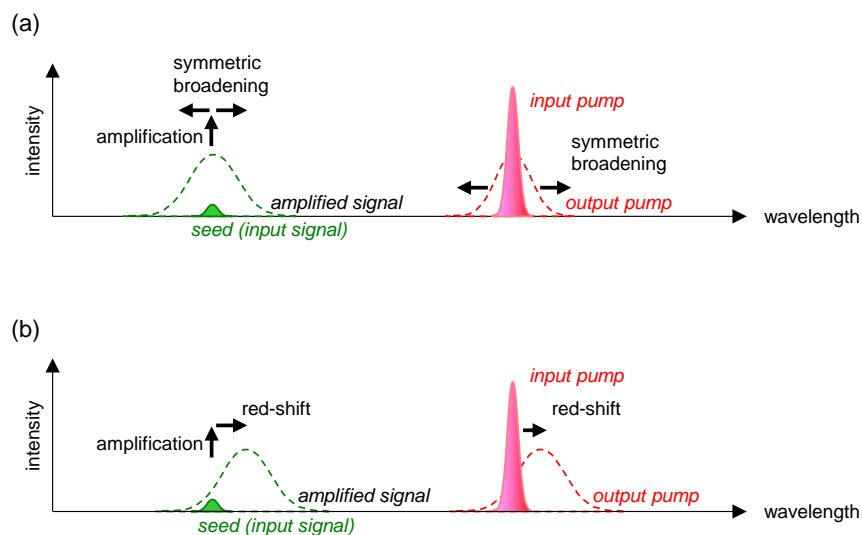

Figure 1. The schematic drawing of the four-wave optical parametric amplification (FWOPA) in (**a**) Raman-inactive and (**b**) Raman-active media. The wavelength of the signal pulse is assumed to be shorter than the wavelength of the pump pulse as in the experimental condition in this research.

3. Experimental Investigation

For the experimental observation of the above spectral shift during the FWOPA, an experimental setup similar to that described elsewhere was employed [11]. As shown in Figure 2, a small portion of the output pulse from a Ti:sapphire chirped-pulse amplifier (CPA, 1 kHz, 1 mJ, 100-fs, 784 nm, Concerto, Thales) was focused into a sapphire plate with a thickness of 3 mm for the generation of a white-light continuum. The continuum served as an input signal (seed) pulse for seeding the FWOPA, while the remaining part of the near-infrared (NIR) pulse was used as a pump pulse. The pump pulse was sent to an optical delay line after being passed through a variable neutral-density filter. The two pulses were then spatially combined by a dichroic mirror reflecting the pump wavelength component while transmitting the signal pulse, and were focused into a hollow fiber (single-hollow-core capillary made of fused silica, a core diameter of 140 μm, an outer diameter of 1.6 mm, 0.5 m long) using an

aluminum-coated concave mirror with a focal length of 500 mm. Two types of gas media were utilized for filling the core of the hollow fiber: argon gas (Raman-inactive gas) and air (Raman-active gas). For the argon gas, the hollow fiber was placed in a vacuum chamber with a gas pressure of 0.7 bar equipped with fused-silica windows with a thickness of 0.5 mm. The gas pressure has given a large amplification gain as reported elsewhere [11]. For the air, the hollow fiber was put in the atmosphere and the pressure was 1 bar. After being separated from the pump pulse by a dichroic mirror, the signal pulse emerging from the hollow fiber was focused into a multi-channel spectrometer for spectral measurement (USB2000, Ocean Optics) using an aluminum-coated concave mirror with a focal length of 200 mm.
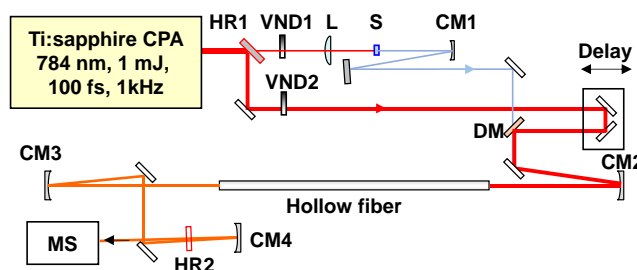
Figure 2. The experimental setup. HR 1,2, high reflector at the pump wavelength; VND 1,2, variable neutral-density filter; L, plano-convex lens (*f* = 60 mm); S, sapphire plate; CM 1–4, concave mirrors, *f* = 100 mm (CM 1), 500 mm (CM 2,3), 200 mm (CM 4); DM, dichroic mirror; MS, multi-channel spectrometer.

4. Results and Discussion

In the FWOPA induced with a gas-filled hollow fiber, it is possible to balance the material phase mismatch and the modal phase mismatch by properly selecting the core diameter of the hollow fiber [21]. The core diameter of the air-filled hollow fiber of 140 μm used in the experiment leads to a small linear phase mismatch over signal wavelengths of 600–784 nm for the pump and signal pulses propagating as the fundamental mode of EH_{11}. This estimation is based on the wavelength dependence of the linear phase mismatch calculated by taking into account the dispersion of the refractive index of air [22] and the waveguide dispersion [23]. The core diameter of 140 μm is also appropriate for the FWOPA in the argon-filled hollow fiber at the similar gas pressure [11]. For a high-order mode to be involved in the interaction of the FWOPA, a much higher gas pressure than the present experiment or combination of high-order modes is necessary: the latter results in amplification only at a specific signal wavelength [11]. In the experiment, the beam diameters of the input pump pulses were carefully adjusted by choosing the appropriate focusing mirror to couple the input beams into the EH_{11} mode and not to induce a high-order propagation mode. The beam diameter of the pump pulse was 120 μm at the entrance of the fiber. The output beams projected on a white screen had Gaussian-like spatial intensity distributions, including the pump pulse and the signal pulses with and without the amplification by the FWOPA. This indicates that the FWOPA in the present study was induced by the EH_{11} propagation mode. The estimated pulse energy of the signal pulse launched into the hollow fiber was less than one nanojoule. The input signal pulse contained continuous spectral components from 450 nm to 700 nm and the bandwidth was much broader than that of the pump pulse as in the previous research [11]. The pulse duration of the signal pulse was

also longer than the pump-pulse duration, and the signal pulse was positively chirped. The pulse duration of the signal pulse was estimated to be about 700 fs in the hollow fiber from the data of the delay-dependent spectral change in the signal pulse which will be discussed later. Only a limited portion of the spectral components in the signal pulse hence temporally overlapped with the pump pulse for the induction of the FWOPA. The wavelength of the overlapped signal spectral component increased with an increase in the time delay of the signal pulse with respect to the pump pulse.

4.1. Spectral Redshift during Signal Amplification

The wavelength of the signal pulse overlapped with the pump pulse was adjusted to around 560 nm. In the argon-filled hollow fiber, the signal pulse was frequency modulated as shown in Figure 3a as a result of the XPM induced by the pump pulse with an energy of 150 μJ. The spectral intensity of the signal pulse decreased at around 560 nm and increased at around 510 nm and 610 nm, resulting in nearly bilaterally symmetric spectral modulation. This is consistent with the spectral characteristic that is expected for the XPM discussed above. When the pump pulse energy was increased to 470 μJ, the signal pulse energy increased by the FWOPA as shown in Figure 3b. The center of gravity of the amplified spectral components did not change from 560 nm during the amplification. This is consistent with the expected characteristics for the FWOPA in a Raman-inactive medium discussed in above.
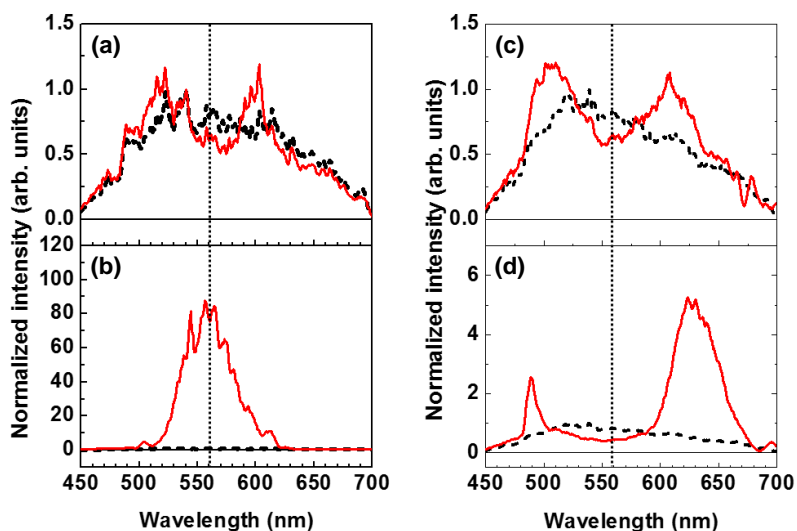

Figure 3. Spectra of output signal pulses from (**a**,**b**) the argon-filled hollow fiber and (**c**,**d**) air-filled hollow fiber. Solid lines and broken lines are the spectra obtained with and without use of the pump pulse, respectively. The energy of the pump pulse was 150 μJ for (**a**) and (**c**), while 470 μJ and 310 μJ for (**b**) and (**d**), respectively. All the spectra are normalized to the peak intensity of the output signal spectrum obtained without use of the pump pulse.

For the air-filled hollow fiber, the spectrum of the signal pulse was as shown in Figure 3c when the pump pulse with an energy of 150 μJ was focused into the hollow fiber together with the signal pulse. The characteristics of the spectral modulation were similar to those observed for the argon gas, and the signal pulse would have been modulated mainly by the XPM. The signal pulse was amplified when the pump pulse energy was increased. The spectrum of the signal pulse emerging from the air-filled hollow fiber changed to that shown in Figure 3d with the increase of the pump energy to 310 μJ. The spectral

characteristics in the amplification were different from those observed for the argon-filled hollow fiber. The energy of the signal pulse increased mainly at long wavelengths around 630 nm which was longer than the wavelength of the spectral component temporally overlapped with the pump pulse (around 560 nm). The wavelength of the spectral peak continuously increased with an increase in the pump pulse energy.

4.2. Excitation of Rotational Wavepackets by the Pump Pulse and the Signal Modulation

To investigate if the above spectral redshift during the amplification related to a coherent motion induced by the pump pulse, the spectrum of the output pump pulse was measured as shown in Figure 4. When the pulse energy of the pump pulse increased from 150 μJ to 310 μJ, a part of the pump spectrum continuously shifted to long wavelengths to form a spectral peak at 822 nm when the energy reached 310 μJ or the center of gravity of the spectrum of the pump pulse shifted to the longer wavelength. The spectral redshift of the pump pulse indicates the generation of coherent motion [13,14]. Since the pump pulse duration was shorter than the periods of molecular rotations of the nitrogen and oxygen contained in air, the coherent rotational wavepackets of these molecules would have been excited.
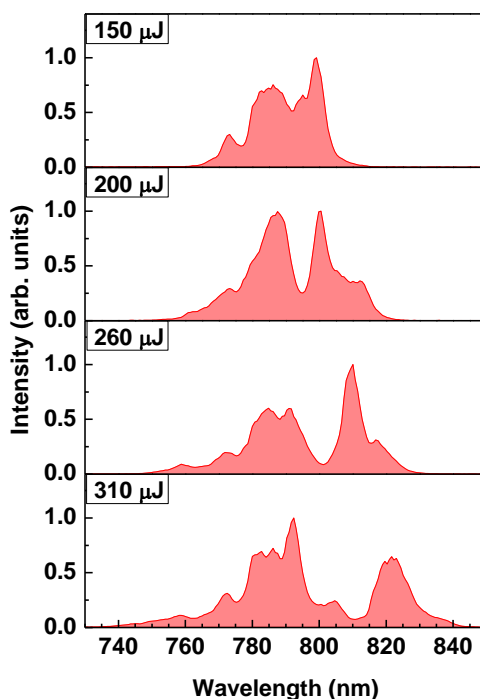

Figure 4. Spectra of the output pump pulses from the air-filled hollow fiber at pump energies of 150, 200, 260, and 310 μJ, respectively. Each spectrum is normalized to its peak intensity.

The excitation of the rotational wavepackets was also confirmed by measuring the spectral change in the signal pulse while scanning the time delay of the signal pulse with respect to the pump pulse. For this, the optical path length of the pump pulse was decreased using the delay line in the beam line of the pump pulse shown in Figure 2 to delay the signal pulse. The spectrum of the signal pulse emerging from the hollow fiber was recorded with the spectrometer at various time delays. The delay of the signal pulse was scanned from −0.5 ps to 12 ps with a step size of 70 fs, and the energy of the input pump pulse was 300 μJ. The signal spectrum at a time delay of −0.8 ps was subtracted from all the measured spectra to clearly show the spectral change with the time delay. The resulting two-dimensional difference spectra

Δ*I (λ, τ)* are shown in Figure 5a which are normalized to the peak spectral intensity of the subtracted spectrum. The origin of the time delay (0 ps) was defined as the delay at which the amplified signal spectrum peaked at 610 nm as schematically depicted in Figure 6a. Spectral change was observed even when the signal pulse was completely separated from the pump pulse, for instance, at time delays of around 2, 4, 6, 8, 10, and 12 ps as indicated by Figure 5a,c. The wavelength at which the signal pulse was modulated shifted to a long wavelength with an increase in the time delay of the pump pulse because of the positive frequency chirp of the signal pulse. This periodic spectral modulation with a period of 2 ps is explained by the phase modulation by the revivals of the rotational wavepackets [16,19,24,25]. The period of 2 ps agrees with half the period of the full revival of the molecular alignment of nitrogen molecules [16,19]. There is also spectral modulation at a delay of about 3 ps, indicating the presence of rotational wavepackets of oxygen molecules [19]. The spectral modulation originates from numerous optically allowed rotational Raman transitions excited within the bandwidth of the pump pulse [19].
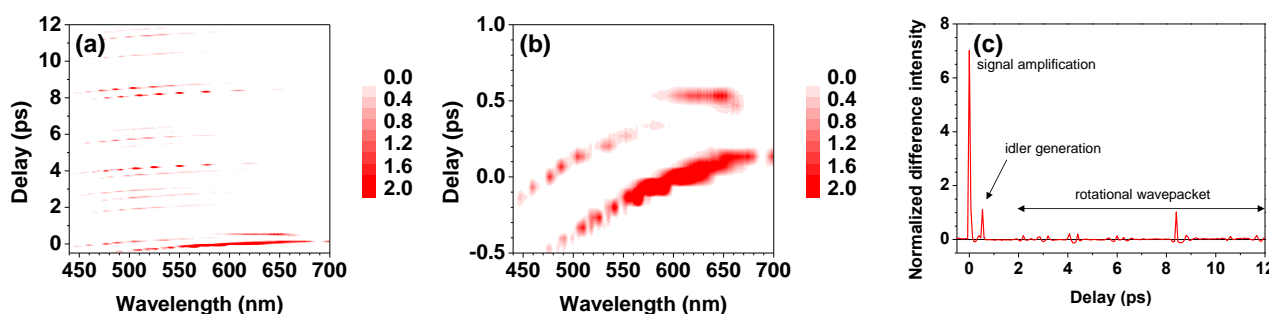

Figure 5. (**a**) The two-dimensional difference spectra of the signal pulse. (**b**) An expanded view of (**a**). (**c**) Delay dependence of the difference intensity at 610 nm in (**a**).

The above observations suggest that the spectral redshift of the pump pulse observed in Figure 4 was due to the phase modulation by the rotational wavepackets of nitrogen in the air, which was excited by the pump pulse. The signal pulse that copropagated with the pump pulse was also phase modulated by the rotational wavepackets at positive time delays. When the pump pulse and the signal pulse were temporally overlapped, the signal pulse would have also been modulated by the wavepackets in addition to experiencing the energy amplification via the FWOPA. The phase modulation would have been the source of the spectral redshift during the amplification of the signal pulse observed in Figure 3d as discussed in the second section.

The phase modulation by the rotational wavepackets alone does not change the energy of the signal pulse. At time delays longer than 1 ps, the signal and pump pulses were completely separated in time from each other as schematically depicted in Figure 6c. No variation of the pulse energy was observed for the signal pulse in the delay range, and only the spectral modulation was observed. At a time delay of 0.53 ps, increase in the energy was observed (see Figure 5b,c). This intensity change was also observed in the Ar-filled hollow fiber, suggesting that it is not arising from the effect of the rotational wavepackets nor the FWOPA seeded by the visible spectral component in the signal pulse. Instead, it was due to the idler generation via the FWOPA seeded by an NIR spectral component (950–1200 nm), which was also contained in the signal pulse as schematically shown in Figure 6b. The NIR spectral component was parametrically amplified via the FWOPA, resulting in the generation of the

corresponding idler spectral components in the visible spectral range (580–670 nm). The NIR spectral component in the input signal pulse was generated in the sapphire crystal and was simultaneously focused into the hollow fiber together with the other spectral component of the signal pulse.
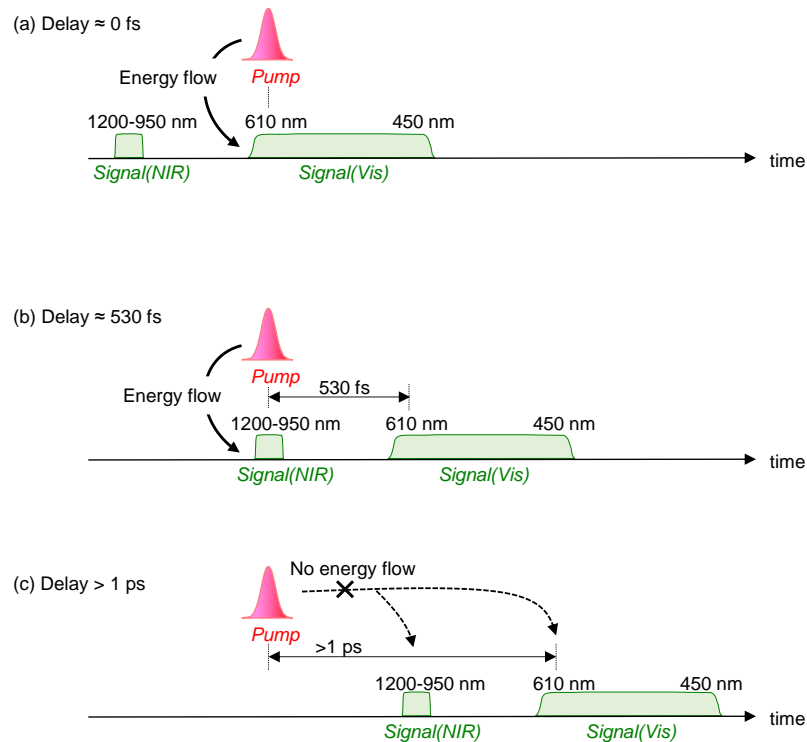
Figure 6. The schematic drawings of the temporal relations between the pump pulse and the signal spectral components at delays around (**a**) 0 fs, (**b**) 530 fs, and (**c**) longer than 1 ps. The input signal contained the near-infrared (NIR) spectral components as discussed in the text.
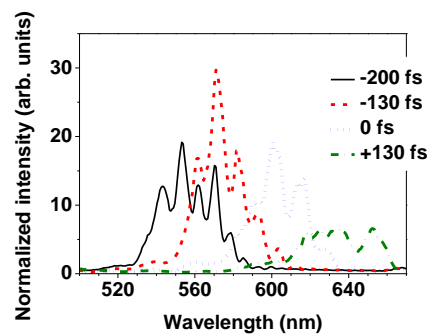
Figure 7. Spectra of the amplified signal pulse at time delays of −200 fs (solid line), −130 fs (broken line), 0 fs (dotted line), and 130 fs (dashed-dotted line). All the spectra are normalized to the peak intensity of the output signal spectrum obtained without use of the pump pulse.

The signal pulse was amplified via the FWOPA within the delay range from −500 to 500 fs, and the peak wavelength of the amplified signal pulse was tunable. Four typical amplified spectra measured at time delays of −200 fs, −130 fs, 0 fs, and 130 fs obtained when using a pump pulse with an energy of 460 µJ are shown in Figure 7. The tunable range of the peak wavelength was from 530 nm to 660 nm,

and the spectral peak intensity increased by up to 30 times by the FWOPA. The amplification rate was lower than that observed for the argon-filled hollow fiber. The rate might be improved by the optimization of the pressure of air for better phase matching or by use of a hollow fiber with other core diameter. The pressure also affects the wavelength range in which the amplification is observed.

Amplification of light has also been reported in previous research using another third-order nonlinearity, stimulated Raman scattering [26–29]. The amplification relies on the nonlinearity originating from the nuclear response of molecules. For the amplification via stimulated Raman scattering, the frequency separation between the pump pulse and the seed pulse being amplified needs to be matched to the Raman shift, and the frequency of the seed pulse needs to be lower than that of the pump pulse. When the pulse duration of the pump pulse is shorter than a molecular motional period, the dynamics changes to impulsive stimulated Raman scattering that continuously shifts the frequency of the short pump pulse to a lower frequency. This was observed in previous researches [13,14,19] and in the present research as shown in Figure 4. This process does not require any phase matching.

Contrary to the amplification by stimulated Raman scattering, the amplification of light in the present research relies on the nonresonant FWM [10,11] that originates from the instantaneous response of the bound electrons rather than the nuclear response. The FWOPA poses no limitation on the frequency separation between the two input pulses, pump and signal pulses, except that the signal frequency must be lower than twice the pump frequency. The signal frequency can be both lower and higher than that of the pump pulse, and the FWOPA involves an energy flow from the pump pulse into the signal pulse being amplified and that into the idler pulse. The phase matching condition needs to be satisfied in this process. When the FWOPA is induced in a Raman medium and the nuclear response discussed above is simultaneously excited through impulsive stimulated Raman scattering, the excited nuclear response redshifts the signal frequency during the amplification as observed in the present research. When the signal pulse is delayed with respect to the pump pulse, no energy flow from the pump pulse into the signal pulse occurs. Only the frequency modulation of the signal pulse by the nuclear response is observable as in Figure 5, and as observed in the previous reports [13–16,18,19,24,25]. The Raman resonant FWM [30–35] may also be employed for the FWOPA. The amplification in this case would be observable only at a specific signal wavelength determined by the Raman shift. When an additional Raman mode is impulsively excited other than the Raman mode responsible to the FWOPA, the spectral redshift may also be induced during the signal amplification.

5. Conclusions

In conclusion, the FWOPA in a Raman-active gas has been investigated by utilizing an air-filled hollow fiber. Rotational wavepackets of molecules are excited by a femtosecond pump pulse during the FWOPA. The phase modulation by the rotational wavepackets leads to a spectral redshift of the signal pulse during the amplification as well as a spectral redshift of the pump pulse. The magnitude of the shift depends on the pump energy which determines the amplitude of the coherent motion being excited. The spectral shape of the amplified signal pulse is therefore not determined only by the FWOPA process, but is also affected by the response of the wavepackets as well as SPM and XPM. The FWOPA in the Raman-active gas produces an amplified signal pulse with a center wavelength that is longer than that

of the signal pulse amplified in a Raman-inactive medium. The magnitude of the shift depends on the intensity of the pump pulse inducing the FWOPA.

Author Contributions

Y.K. conceived and designed the experiments; Y.K. performed the experiments; Y.K. analyzed the data; T.I. contributed experimental tools; Y.K. wrote the paper.

Conflict of Interest

The authors declare no conflict of interest.

References

1. Shirakawa, A.; Sakane, I.; Kobayashi, T. Pulse-front-matched optical parametric amplification for sub-10-fs pulse generation tunable in the visible and near infrared. *Opt. Lett*. **1998**, *23*, 1292–1294.
2. Baltuska, A.; Fuji, T.; Kobayashi, T. Visible pulse compression to 4 fs by optical parametric amplification and programmable dispersion control. *Opt. Lett*. **2002**, *27*, 306–308.
3. Herrmann, D.; Homann, C.; Tautz, R.; Scharrer, M.; Russell, P.S.J.; Krausz, F.; Veisz, L.; Riedle, E. Approaching the full octave: Noncollinear optical parametric chirped pulse amplification with two-color pumping. *Opt. Express* **2010**, *18*, 18752–18762.
4. Harth, A.; Schultze, M.; Lang, T.; Binhammer, T.; Rausch, S.; Morgner, U. Two-color pumped OPCPA system emitting spectra spanning 1.5 octaves from VIS to NIR. *Opt. Express* **2012**, *20*, 3076–3081.
5. Witte, S.; Zinkstok, R.T.; Hogervorst, W.; Eikema, K.S.E. Generation of few-cycle terawatt light pulses using optical parametric chirped pulse amplification. *Opt. Express* **2005**, *13*, 4903–4908.
6. Herrmann, D.; Veisz, L.; Tautz, R.; Tavella, F.; Schmid, K.; Pervak, V.; Krausz, F. Generation of sub-three-cycle, 16 TW light pulses by using noncollinear optical parametric chirped-pulse amplification. *Opt. Lett*. **2009**, *34*, 2459–2461.
7. Schmid, K.; Veisz, L.; Tavella, F.; Benavides, S.; Tautz, R.; Herrmann, D.; Buck, A.; Hidding, B.; Marcinkevicius, A.; Schramm, U.; *et al.* Few-cycle laser-driven electron acceleration. *Phys. Rev. Lett.* **2009**, *102*, doi:10.1103/PhysRevLett.102.124801.
8. Dubietis, A.; Tamosauskas, G.; Polesana, P.; Valiulis, G.; Valtna, H.; Faccio, D.; Di Trapani, P.; Piskarskas, A. Highly efficient four-wave parametric amplification in transparent bulk Kerr medium. *Opt. Express* **2007**, *15*, 11126–11132.
9. Valtna, H.; Tamosauskas, G.; Dubietis, A.; Piskarskas, A. High-energy broadband four-wave optical parametric amplification in bulk fused silica. *Opt. Lett.* **2008**, *33*, 971–973.
10. Faccio, D.; Grün, A.; Bates, P.K.; Chalus, O.; Biegert, J. Optical amplification in the near-infrared in gas-filled hollow-core fibers. *Opt. Lett.* **2009**, *34*, 2918–2920.

11. Kida, Y.; Imasaka, T. Optical parametric amplification of a supercontinuum in a gas. *Appl. Phys. B* **2013**, *116*, 673–680.

12. Yan, Y.-X.; Gamble, E.B.; Nelson, K.A. Impulsive stimulated scattering: General importance in femtosecond laser pulse interactions with matter, and spectroscopic applications. *J. Chem. Phys.* **1985**, *83*, 5391–5399.

13. Korn, G.; Dühr, O.; Nazarkin, A. Observation of Raman Self-Conversion of fs-Pulse Frequency due to Impulsive Excitation of Molecular Vibrations. *Phys. Rev. Lett.* **1998**, *81*, 1215–1218.

14. Wittmann, M.; Nazarkin, A.; Korn, G. New regime of fs-pulse stimulated Raman scattering. *Appl. Phys. B* **2000**, 70, 261–267.

15. Bartels, R.A.; Weinacht, T.C.; Wagner, N.; Baertschy, M.; Greene, C.H.; Murnane, M.M.; Kapteyn, H.C. Phase Modulation of Ultrashort Light Pulses using Molecular Rotational Wave Packets. *Phys. Rev. Lett.* **2001**, *88*, doi:10.1103/PhysRevLett.88.013903.

16. Noack, F.; Steinkellner, O.; Tzankov, P.; Ritze, H.-H.; Herrmann, J.; Kida, Y. Generation of sub-30 fs ultraviolet pulses by Raman induced phase modulation in nitrogen. *Opt. Express* **2005**, *13*, 2467–2474.

17. Darginavičius, J.; Tamošauskas, G.; Valiulis, G.; Dubietis, A. Broadband four-wave optical parametric amplification in bulk isotropic media in the ultraviolet. *Opt. Commun.* **2009**, *282*, 2995–2999.

18. Ripoche, J.-F.; Grillon, G.; Prade, B.; Franco, M.; Nibbering, E.; Lange, R.; Mysyrowicz, A. Determination of the time dependence of N_2 in air. *Opt. Commun.* **1997**, *135*, 310–314.

19. Nibbering, E.; Grillon, G.; Franco, M.A.; Prade, B.S.; Mysyrowicz, A. Determination of the inertial contribution to the nonlinear refractive index of air, N_2, and O_2 by use of unfocused high-intensity femtosecond laser pulses. *J. Opt. Soc. Am. B* **1997**, *14*, 650–660.

20. Diels, J.-C.; Rudolph, W. *Ultrashort Laser Pulse Phenomena*, 2nd ed.; Academic Press: San Diego, CA, USA, 2006.

21. Durfee, C.G.; Misoguti, L.; Backus, S.; Kapteyn, H.C.; Murnane, M.M. Phase matching in cascaded third-order processes. *J. Opt. Soc. Am. B* **2002**, *19*, 822–831.

22. Peck, E.R.; Reeder, K. Dispersion of Air. *J. Opt. Soc. Am.* **1972**, *62*, 958–962.

23. Marcatili, E.A.J.; Schmeltzer, R.A.R. Hollow Metallic and Dielectric Waveguides for Long Distance Optical Transmission and Lasers. *Bell Syst. Tech. J.* **1964**, *43*, 1783–1809.

24. Calegari, F.; Vozzi, C.; Gasilov, S.; Benedetti, E.; Sansone, G.; Nisoli, M.; De Silvestri, S.; Stagira, S. Rotational Raman Effects in the Wake of Optical Filamentation. *Phys. Rev. Lett.* **2008**, *100*, doi:10.1103/PhysRevLett.100.123006.

25. Calegari, F.; Vozzi, C.; Stagira, S. Optical propagation in molecular gases undergoing filamentation-assisted field-free alignment. *Phys. Rev. A* **2009**, *79*, doi:10.1103/PhysRevA.79.023827.

26. Krylov, V.; Rebane, A.; Erni, D.; Ollikainen, O.; Wild, U.; Bespalov, V.; Staselko, D. Stimulated Raman amplification of femtosecond pulses in hydrogen gas. *Opt. Lett.* **1996**, *21*, 2005–2007.

27. Vodchits, A.I.; Shvedko, A.G.; Orlovich, V.A.; Kozich, V.P.; Werncke, W. Stimulated Raman amplification of ultrashort seed pulses in compressed methane. *J. Opt. Soc. Am. B* **2005**, *22*, 453–458.

28. Abdolvand, A.; Nazarkin, A.; Chugreev, A.V.; Kaminski, C.F.; Russell, P.S.J. Solitary Pulse Generation by Backward Raman Scattering in H_2-Filled Photonic Crystal Fibers. *Phys. Rev. Lett.* **2009**, *103*, doi:10.1103/PhysRevLett.103.183902.

29. Trabold, B.M.; Abdolvand, A.; Euser, T.G.; Walser, A.M.; Russell, P.S.J. Amplification of higher-order modes by stimulated Raman scattering in H_2-filled hollow-core photonic crystal fiber. *Opt. Lett.* **2013**, *38*, 600–602.

30. Imasaka, T.; Kawasaki, S.; Ishibashi, N. Generation of more than 40 laser emission lines from the ultraviolet to the visible regions by two-color stimulated raman effect. *Appl. Phys. B* **1989**, *49*, 389–392.

31. Yavuz, D.; Walker, D.; Shverdin, M.; Yin, G.; Harris, S.E. Quasiperiodic Raman Technique for Ultrashort Pulse Generation. *Phys. Rev. Lett.* **2003**, *91*, doi: 10.1103/PhysRevLett.91.233602.

32. Sali, E.; Mendham, K.J.; Tisch, J.W.G.; Halfmann, T.; Marangos, J.P. High-order stimulated Raman scattering in a highly transient regime driven by a pair of ultrashort pulses. *Opt. Lett.* **2004**, *29*, 495–497.

33. Sensarn, S.; Goda, S.N.; Yin, G.Y.; Harris, S.E. Molecular modulation in a hollow fiber. *Opt. Lett.* **2006**, *31*, 2836–2838.

34. Bauerschmidt, S.T.; Novoa, D.; Abdolvand, A.; Russell, P.S.J. Broadband-tunable LP_{01} mode frequency shifting by Raman coherence waves in a H_2-filled hollow-core photonic crystal fiber. *Optica* **2015**, *2*, 536–539.

35. Motoyoshi, K.; Kida, Y.; Imasaka, T. High-Energy, Multicolor Femtosecond Pulses from the Deep Ultraviolet to the Near Infrared Generated in a Hydrogen-Filled Gas Cell and Hollow Fiber. *Appl. Sci.* **2014**, *4*, 318–330.